Effect on Structural and Magnetic properties of nano Lithium Zinc Aluminates by the dopant Fe^{3+} synthesized by co-precipitation method for Microwave observing material in communication system and for Opto-magnetic application

Uthayakumar. B[1], *Sukandhiya. S[2], Suryakumary. J[3], S. Periandy[4]

[1,2,3](Research Scholar, Department of Physics, Kanchi Mamunivar center for PG Studies, Puducherry, India.)
[4](Associate Professor, Department of Physics, Kanchi Mamunivar center for PG Studies, Puducherry, India.)
*(Corresponding Author Email id : Sukandhiya2010@gmail.com
Corresponding Author: Sukandhiya. S)

Abstract: *Nano Lithium-Zinc Aluminate is doped with Fe ion in concentration of (x =0, 0.5,1.5,2.0) synthesized by Co-Precipitation method. Impact of Fe dopant in nano $Li_{1.0}Zn_{0.5}Fe_xAl_{2-x}O$ has been investigated and reported in the present paper. Precipitates are obtained at bath pH as 10 and bath temperature as 338K. Samples are sintered at 1173K before characterization. X-ray diffraction analysis done with X-ray Diffractometer (XRD) to find structural parameters such as lattice constant, crystallite size, lattice strain, X-ray density and dislocation density. Crystallite size increase with increase in Fe^{3+} ion and it lies between 33nm and 51 nm. Lattice constant also increases with increase in dopant and it ranges between 8.1563Å and 8.5606Å. Morphology and composition of the prepared samples are observed with Scanning Electron Microscope (SEM) and Energy Dispersive Spectrometer (EDS) respectively. From SEM, morphology of the sample changes from agglomerated to crystalline form on increase in Fe dopant. Fourier Transform Infrared spectroscopy reveals that Fe doped samples show two strong absorption bands in the range of 600-400 cm^{-1} which confirm the presence of metal-oxygen stretching band in ferrite. Vibration sample magnetometer (VSM) is used to investigate magnetic parameters Saturation Magnetization M_s, Remanent Magnetization M_r, Coercivity H_c, and Magneto crystalline Anisotropy K and magneton number. Maximum K value 462.82erg and M_s 80.072 emu/g obtained for x= 1.5.*

Keywords - *Opto-Magnetic, Li-Zn-Fe Aluminates, EDS, FTIR, SEM, VSM, XRD*

I. Introduction

Spinel Zinc Aluminate $ZnAl_2O_4$, designated as gahnite, is a ceramic semiconductor with band gap of about 3.9 eV and it is chemically and thermally stable material. It is commonly used as catalyst or support in many catalytic reactions such as cracking, dehydrogenation, acetylation and transestrification When it is doped with transition metal ions it will exhibit luminescence property Nano size of their bulk parts has wide range of application such as magnetic, optical, ceramics and catalysis [1]. If doping Lithium with gahnite will enhance the electrical property of the combination. Lithium aluminates are also most wanted candidate for counter parts of Lithium batteries and also used as tritium breeding material in fusion reactors [2], it is low cost substitution for garnets. Iron is most abundant metals in earth crust. Further, the combination of Li-Zn Aluminates is doped with 'Fe' dopant with the composition, it avails magnetic property in addition to that. The general formula of spinels is AB_2O_4. In the spinel structure, the anions are arranged in a cubic close packed array with the cations arranged in the holes of the array. It is constructed by 8 tetrahedral and 4 octahedral holes per molecule. Further spinel are classified into normal, inverse and mixed spinel according to the occupancy of cations. In normal spinels A^{2+} ions occupy tetrahedral holes and B^{3+} ions are present in the octahedral holes. In inverse spinels, one half of A^{2+} ions occupy tetrahedral holes and the remainder of A^{2+} ions and all B^{3+} ions in octahedral holes. In mixed spinel both cations present in tetrahedral and octahedral sites [3]. Nano spinel Li-Zn ferrites have been found to be excellent material in permanent magnets, high density recording media, absorbers and microwave devices due to their low costs, high resistivity and low eddy current loss [4-6]. Few works are have been done to modify the magnetic parameters of Li-Zn ferrites by substituting Fe^{3+} with other cation. [7-9] Present work is to tailor potential novel combination for electrical and magnetic application. To achieve this Iron doped with Lithium-Cobalt Aluminates synthesized by co-precipitation.

II. Materials and Methods

2.1 Material for synthesis

$Li_{1.0}Zn_{0.5}Fe_xAl_{2-x}O_4$ nano Aluminates at various concentration of iron ion has been synthesized from Precursors $LiCl$, $ZnCl_2$, $AlCl_3$, $FeCl_3.6H_2O$ and $NaOH$. Analytical grade of these precursors are purchased from SIGMA ALDRICH, Germany with 98% purity.

2.2 Synthesis Methodology

A productive synthesizing methodology depends on starting material, and its composition. Environment of reaction carried out also plays an important role. Wet chemical methods like co-precipitation, sol-gel, hydrothermal and colloid emulsion technique, pH plays an important role. For the present investigation eco friendly NaOH is used to maintain pH. The physio-chemical properties of nanoparticles are greatly influenced by particle size, morphology, purity and chemical composition. Using chemical methods, have been conformed to efficiently control the morphology and chemical composition of prepared nano powder. Among wet chemical techniques sol-gel, hydro thermal and colloid emulsions are time consuming and involve highly unstable alkoxides and difficult to maintain reaction conditions. Co-precipitation is one of the more successful techniques for synthesizing ultrafine nanoparticles having narrow particle size distribution [9]. These advantages on co-precipitation method motivated authors to synthesize $Li_{1.0}Zn_{0.5}Fe_xAl_{2-x}O_4$ (x = 0, 0.5, 1.5, 2.0) nano aluminates by co-precipitation method. The precursors for Fe ion is taken as 2 M and 1M for other Metals chlorides. They are mixed in stochiometric ratio and added one by one on the basis of their electro-negativity value. combination of Aqueous solution is stirred rigorously at 338K for 30 minutes, mean while NaOH is added to the brain solution by drop by drop using a burette till solution reaches pH value 10. The required composition of nano ferrites are formed from conversion of metal salt into hydroxide and then transformed into ferrites. The precipitates obtained were thoroughly washed more than three times with double distilled water and acetone. For the present work as synthezied sample and samples sintered at 1173 K are considered for study.

2.3 Physical measurements

Crystal structure of all the samples were examined by powder X-Ray diffraction XRD patterns at room temperature PANalytical-X'Pert PRO powder diffractometer using Cu-$K_{\alpha 1}$ radiation. Scanning Electron Microscopy (SEM) study was performed by VEGA 3 TESCAN Scanning Electron Microscope, operated at 120 KV. Elemental analysis has been done with BRUKER EDS. Fourier Transform Infrared (FT-IR) spectra were recorded on SHIMADZU FT-IR spectrophotometer using KBr pellets in the range 4000-400 cm^{-1}. The magnetic properties were measured at room temperature by LAKESHORE vibrating sample magnetometer (VSM).

III. Result and Discussion

3.1 X - Ray Diffraction analysis

X-ray diffraction pattern of synthesized samples of Fe doped Lithium-Zinc nano spinel Aluminates for the concentration x = 0, 0.5, 1.5 and 2.0 sintered at 1173K are shown in the Fig.1. Major peaks (220), (311), (400), (511), (440), (620) and (533) are present in XRD pattern of all the samples which reveals these are having the disordered spinel ferrite formation of space group Fd3m, with Fe^{3+} in tetrahedral (8c) and octahedral (12d) sites whereas Al^{3+}, Li^+ and Zn^{2+} ions occupy the octahedral position [10]. This matches with the ($ZnAl_2O_4$) JCPDS file No.05-0669, $Li_{0.5}Fe_{2.5}O_4$ JCPDS file.No.88-0671, $ZnFe_2O_4$ JCPDS file No. 01-1121 [11, 12]. Minor peak 422 present in all sample except x = 2 and 620 peak present in all samples x = 0.5 and 1.5. Absence of 422 and 620 represents the samples having amorphization samples[13]. The extra peak (310) is observed only in x = 2 and (330) is present only in x= 0.5 which represents presence of α-Lithia in the sample. Generally intensity of XRD peaks confirms the crystalline nature of the samples. Addition of Iron with Lithium-Zinc Aluminates increase the crystalline nature of samples it results in increases intensity of XRD peaks. Peaks of XRD pattern shift towards higher diffraction angle, this is due to replacement of smaller ionic radius Al^{3+} ion (r_{Al} = 0.51 Å) by bigger ionic radius Fe^{3+} ion (r_{Fe} = 0.64 Å) in Li-Zn nano Aluminates. Intensity of (220) decreases and (311) increases with increasing Fe content in the sample. Addition of iron ion will supplies both Fe^{2+} and Fe^{3+} for tetrahedral and octahedral sites to have a stable cation distribution. From fig 1. the prominent peaks shift towards lower angle which results in increase of lattice constant. The intensities of (220) and (440) planes are more sensitive to cations in tetrahedral and octahedral sites respectively [14, 15]. From TABLE 1 it is clear that intensity of (440) decrease with increasing Fe^{3+} and this expressing decreasing Al^{3+} ions in the octahedral sites. Intensity found to reverse for the concentration x = 2 this may be due to absence of Al^{3+} ions in this ratio. Decrease in intensity of (220) peak maybe due to replacement of Fe^{2+}, Fe^{3+} instead of Al^{3+} and migration of Li^+ ions from octahedral site to tetrahedral site vice versa. Average crystallite size 'D' and lattice constant has been estimated from X-ray reflections indexed (220), (311), (400), (422), (511) (440) (620) and (533) using Scherer's equation D = 0.9 λ / β cos θ , where D is the average crystallite size, β is the full width

half maxima, λ is the X-Ray wavelength and θ is the Bragg's angle [16]. Lattice constant has been calculated from equation a = d $(h^2 + k^2 + l^2)^{1/2}$ Where 'a' is lattice constant, d be the inter planar distance, hkl is miller indices. Lattice strain of $Li_{1.0}Zn_{0.5}Fe_xAl_{2-x}O_4$ (x = 0, 0.5, 1.5, 2.0) nano aluminates were determined using the Williamson-Hall formula ε = β / 4 tan θ, Where ε is the lattice strain of the structure [17, 18]. X-ray Density can be calculated by ρ_x = ZM/Na^3, Where Z is number of molecules per unit cell, here it is 8. M is Molecular weight of the sample N is Avagadro's Number, 'a' lattice constant. Dislocation density has been found by using the relation δ = 15 ε / a D, here δ be the dislocation density. All these structural parameters are calculated and tabulated in TABLE 2. The average crystallite size 'D' and lattice constant gets increases with increasing by adding higher ionic radius Fe^{3+}ion (r_{Fe} = 0.67 Å) instead of lower ionic radius Al^{3+} ion (r_{Al} = 0.51 Å) and values lies between 33nm and 50nm. For x= 0.5 the average crystallite size is less in comparison to x= 0 this may be due to the migration of Zn^{2+} (r_{Al} = 0.82 Å) to octahedral and Fe3+ (r_{Fe} = 0.67 Å)) to tetrahedral sites (A). In nano regime, it is possible that some of Zn^{2+} ions may migrate towards octahedral site. Lattice constant also increases with incorporation of Fe ion instead of Al ion and their values are 8.1563 Å to 8.5606 Å. This linear variation in 'D' and 'a' reveals that replacement of Al ion by Fe obeys the Vegard's law. Increase in molecular weight of the $Li_1Zn_{0.5}Al_xFe_{2-x}O_4$ composition and increase in X-Ray density values are due to replacement of higher atomic mass Fe^{3+} (55.84 gm) by lower atomic mass Al^{3+} (26.98 gm). More crystallite size present at x=2 having least lattice strain and least dislocation density value.

3.2 Scanning Electron Microscope (SEM) and Energy Dispersive Spectroscopic (EDS) analysis

External morphology of synthesized samples of $Li_{1.0}Zn_{0.5}Fe_xAl_{2-x}O_4$ (x = 0, 0.5, 1.5, 2.0) nano aluminates sintered at 1173 K have been investigated with the help of VEGA 3 TESCAN for all concentration of the samples as shown in Fig.2. The micrographs show the agglomerated grains with clusters of fine particle in the composition for x = 0, 0.5, 1.5. The morphology is almost uniform and regular having cubic shaped particles at x = 2.0 only. Replacement of Aluminium by Iron manipulated the morphology [19]. More crystallite size have uniform grain at x=2. The surface of the aluminates samples has a number of fine pores or voids that are attributed to the large amount of Oxygen and chlorine gas liberated during the sintering process. Presence of vacancies results in contraction of Lattice even higher   ionic radius dopant is added to the sample. This observation are obtained for x = 0, 0.5, 1.5 except x = 2.0. [20].

EDS spectrum for the $Li_{1.0}Zn_{0.5}Fe_xAl_{2-x}O_4$ (x = 0, 0.5, 1.5, 2.0) nano aluminates are recorded with BRUKER EDS and illustrated in Fig.3. This figure shows each peak corresponds to the element added in the prepared nanoferrite which confirmed the presence of elements in respective concentration. Aluminium and iron are the major constituents in the composition. Oxygen, Lithium and Zinc are the next major constituent in the sample. Peak for Lithium is not obtained in EDS spectra because Silicon detector used in Energy Dispersive X-Ray spectroscope for present study is not having sensing ability to detect small amount of energy emitted by very small Lithium ion which is having K shell for auger electron. It is interesting to note that the preparation condition completely favours the formation of mixed ferrite and allow us to study the effect of increasing the Fe content on the properties of the Fe doped Li-Zn nano Aluminates. The peak values variation is due to it stochiometry, for all the concentration. The values of Aluminium vary with the increase in Iron concentration.

3.3. Fourier Transform Infrared Spectroscopy (FTIR) Analysis

FTIR spectrum of the Fe doped Lithium Zinc Nanoaluminate are shown in Fig.4. Infrared spectroscopy study supported the formation of Fe doped Li Zn Al spinel nano Aluminates with informative of two strong absorption bands around 400 cm^{-1} and 600 cm^{-1} that are common features of all spinel structure [21]. The spinel structure are attributed to the stretching vibrations of the unit cell of the spinel in the tetrahedral (A) site and the metal-oxygen vibration in the octahedral (B) site. These absorption bands are highly sensitive to changes in interaction between oxygen and cations, as well as to the size of the obtained nano-particles [22]. The broadening of the spectral band depends on the statistical distribution of cations over A and B sites. The vibration frequency depends on the cation mass, cation-oxygen distance and bending force [23]. From Fig 4 and Table 3, Intrinsic stretching vibration frequency of metal- oxygen at tetrahedral site observed in a range 665 cm^{-1} - 557 cm^{-1} and its value shifting linearly toward lower frequency with increase in Fe^{3+} concentration. And replacement of Al^{3+} ions by larger atomic mass Fe^{3+} in octahedral sites also results in a decrease in metal oxygen bond length and the values are 517 cm^{-1} - 400 cm^{-1} and consequently decrease the wave number of octahedral and tetrahedral sites by increasing substitution content [24, 25]. Additional subsidiary peak observed at 432.97cm^{-1} at x= 2.0 concentration. After adding the dopant Fe in the concentration tetrahedral site band is obtained. Intensity of the band corresponds to octahedral and tetrahedral site increases upto x= 1.5. Pure LiZn nanoferrite at x= 2.0 have lower intensity compared with x=0.5 and 1.5. It is well known that the intensity ratio is function of change of dipole moment with the internuclear distance. This value represents the contribution of ionic bond Fe-O in the lattice. So the observed increase and decrease in the absorption band intensity with increase in Fe content, is due to perturbation occurring in Fe-O bonds. The electronic distribution of Fe-O bonds

greatly affected by the dopant Fe^{3+} which is having comparatively bigger radius and high atomic weight Al (26.98amu) and Fe (55.84 amu).

3.4 Vibrational Sample Magnetometer (VSM) analysis

Fe doped $Li_{1.0}Zn_{0.5}Fe_xAl_{2-x}O_4$ nanoaluminates (x = 0, 0.5, 1.5, 2.0) hysteresis loops are recorded with LAKESHORE Vibrational sample magnetometer at 300 K with applied field as 20 KOe are shown in Fig.5. The value of anisotropy constant was calculated from Stoner-Wohlfarth relation as follows $H_c = K/M_s$ [26] ,Where H_c is the coercivity , M_s saturation magnetization and K magnetic anisotropy constant .Calculation of magnetic moment in bohr magneton was carried out using the following relation, n_B = (Molecular Weight × M_S)/5585 [27]. Magnetic parameters saturation magnetization (M_s), Remanence Magnetization (M_r), Coercivity (H_c), Squareness ratio, Magnetic anisotropy constant (K) and magneton number are calculated from Hysteresis loop and tabulated in Table 4.Generally magnetic properties in the prepared sample arise from coupling between spin and orbital angular momentum (L-S coupling) and electron spin (S-S coupling) [28]. In the case of spinel nano magnetic ferrite material magnetic parameters are influenced by cation distribution, colinearity and non colinearity (canting) of spins on their surface, crystallite size and dopant. In the present study undoped Li-Zn-Aluminates have hysteresis loop of paramagnetic nature with M_s value. Doping Fe ions with the composition result in increase in M_s value and decrease in coercivity value. For the concentration 1.5 and 2 shows superparamagnetic behaviour. Maximum magnetization value obtained at x= 1.5, even though pure state of LiZnFe at x=2 the diamagnetic nature of Zn reduce the magnetization value. The hysteresis loop shape varies when increasing Fe in the sample and having very low Coercivity value. Sample which is having more M_s value having high bohr magneton value.

The appearance of super-paramagnetic behaviour indicates that the sample having magneto crystalline anisotropy, which is important to hold magnetic ions in certain direction, has been overcome by thermal energy [29]. The magnetic anisotropy constant non-linearly varies this is due to exchange interaction of A-site and B- site cations. Thus VSM result matches with XRD, SEM and FTIR findings.

IV.   Conclusion

$Li_{1.0}Zn_{0.5}Fe_xAl_{2-x}O_4$ (x = 0, 0.5, 1.5, 2.0) nano aluminates were effectively synthesized by unproblematic and uncomplicated co-precipitation route with average crystallite size lies between 33 nm and 51 nm. Structural and Magnetic properties are investigated for samples sintered at 1173K. Doping Fe ion tailored the structural properties such as Average crystallite size, lattice constant, and X-Ray density increases with increase in Fe content in the sample. Lattice strain remains constant except x= 0. Dislocation density of the synthesized samples decrease in addition of Fe. super structure reflection peaks from XRD analysis suggest that nano crystal lattice having disordered spinel structure in the higher concentration of the dopant. SEM shows morphology manipulated by Fe^{3+} ion in the sample and FTIR observation have fine match with results of XRD and SEM. From VSM analysis and Low concentration of Mn^{2+}induced magnetic ordering and crystal disordering. At higher concentration Cobalt induced most disordered magnetic structure which is found from the magnetic anisotropy constant value. Important finding in this work is 1.5 concentration of Fe doped Lithium Zinc Aluminate has its maximum magnetic anisotropy constant value, which will release more thermal energy in alternating magnetic field. And samples with low coercivity and low remanence value can be used for easy demagnetizing applications.

References

[1]   Duan.X, Pan.M, Yu.F, Yuan.D, *J.Alloys Compd. 509* (2011) 1079-1083.
[2]   B.K.K.uanr, G.P.Srivastava, J.Appl. Phys. 75 (1994) 6115
[3]   Sepleak.V, Bergmann.I, Indris.S, Feldhoff.A, Hahn.H, Becker.K.D, *J.Mater. Chem 21* (2011) 8332
[4]   Pardavi-Harvarth.M, *J.Magn. Magn. Mater. 215* (2000) 171
[5]   Yusoff.A.N, Abdullah.M.H, *J.Magn. Magn. Mater.* 269 (2004) 271
[6]   Yunus.S.M, Fernandez-Baca.J.A, Asgar.A.M, *Physica B 262* (1999) 112
[7]   Sukandhiya.S, Uthayakumar.B, S.Periandy,*IOSR-JAP 9 Issue 4* (2017) 4-12
[8]   Uthayakumar.B,Sukandhiya.S. Periandy.S, *IOSR-JAP 9 Issue 5* (2017*)* 1-8
[9]   Marinca.T.F, Chicinas.I, Isnard.O, Pop.V, Pop.F, *J.Alloy., and compounds, 509* (2011) 7931-7936.
[10]   Sukandhiya.S,Uthayakumar.B, Roja.R, Periandy.S, IOSR-JAP 9 Issue 5 Ver 2 (2017) 52-60 .
[11]   Carta.G, Casarin.M, Habra.E.L, *Electrochemica Acta 50* (2005) 4592-4599.
[12]   Bahgat.M, Farghaly.F.E, Abdel Basir, Fouad.A.O, J. Mate.Process. Tech. 183 (2007) 117-121
[13]   Ammankutty.C.G, Sugunna. S, *J.App.Catal.A Gen 218* (2001) 39
[14]   Ladgaonkar.B.P, Vaigainkar.A.S, *Materials chemisty and physics 56* (1998) 280-283.
[15]   Narasimhan.C.S , Swamy.C.S, *Physica status dolidi 59* (1980) 817
[16]   Culity.B.D, *Elements of X-ray diffraction* Chapter 14 (London, Addison-Wesley publishing company.Inc.,1976) (Chapter 14).
[17]   Wolska. E, Piszora. P, Nowicki.W, Darul. J*, Int.J.Inorganic Mater., 3* (2001), 503-507.
[18]   Williamson.G.K., Hall.W.H, *Acta Metall.1*(1953) 22-31.

[19]   Rahman.S, Nadeem.K, Rehman.M.A, Mumtaz.M, Naeem.S, I.L.Ipst,*Ceram.Int. 39* (2013) 5235-5239
[20]   Prabahar. S, Dhanam. M, *J.Cryst.Growth, 41* 285 (2005) 1-2
[21]   Hashim.M, Alimuddin, Shirsath.S.E, Kumar.S, Kumar.R, Roy.A.S, Shah.J, and Kotnala.R.K, *Journal of alloys and compounds, 549* (2012) 348-357.
[22]   Farid.M, Ahmad.I, Aman.S, Kanwal.M, Murtaza.G, Alia.I, Ishfaq.M, *Journal of Ovonic research 11* (2015) 1
[23]   Wahba.A.M, Mohammad.M.B, *Ceramic International, 40* (2014) 6127-6135
[24]   Boshale.A.G, Chougule.B.K, *Material chemisty and physics 97* (2006) 273
[25]   Smit.J, And H.P.J ijn.*Ferrite* (1959)
[26]   Singh.N, Agrawal.A, Sanghi.S, Singh.P, *Physica B, 406* (2011) 687
[27]   Singhal.S, Chandra.K, *J.Solid state Chem. 180* (2007) 296
[28]   Gabbal.M.A, Angari.Y.M.A, *Material chem. Physics 118* (2009) 153
[29]   Verma.A, Goel.T.C, Meadiratta.R.G, Kishan.P, *Journal of Magnetism and magnetic material 208* (2000) 13-19.

TABLE 1: Comparison of X-Ray Intensity

Fe content 'x'	Composition	I_{220}	I_{440}
0	$Li_{1.0}Zn_{0.5}Al_2O_4$	100.0	33.02
0.5	$Li_{1.0}Zn_{0.5}Al_{1.5}Fe_{0.5}O_4$	57.17	34.17
1.5	$Li_{1.0}Zn_{0.5}Al_{0.5}Fe_{1.5}O_4$	56.35	25.83
2	$Li_{1.0}Zn_{0.5}Fe_2O_4$	35.10	31.88

TABLE 2: Structural parameters of $Li_{1.0}Zn_{0.5}Fe_xAl_{2-x}O_4$ (x=0.0, 0.5, 1.5, 2.0) sintered at 1173K

Fe content 'x'	Composition	Crystallite Size D (nm)	Lattice Constant a (Å)	Molecular Weight g/mole	X-ray Density g/cm³	Lattice Strain 10^{-3}	Dislocation Density 10^{15}
0	$Li_{1.0}Zn_{0.5}Al_2O_4$	35.75	8.1563	157.548	3.857292	2.698	1.9431
0.5	$Li_{1.0}Zn_{0.5}Al_{1.5}Fe_{0.5}O_4$	33.9	8.2616	171.981	4.051688	2.753	1.5565
1.5	$Li_{1.0}Zn_{0.5}Al_{0.5}Fe_{1.5}O_4$	41.5	8.5008	200.846	4.343421	2.757	1.7284
2	$Li_{1.0}Zn_{0.5}Fe_2O_4$	50.29	8.5606	215.278	4.55865	2.027	0.8412

TABLE 3: Vibrational frequency of tetrahedral and octahedral sites

Fe content 'x'	Composition	$\nu_{1\,tetra}$ cm^{-1}	$\nu'_{2\,tetra}$ cm^{-1}	$\nu_{2\,octa}$ cm^{-1}
0	$Li_{1.0}Zn_{0.5}Al_2O_4$	-		456.91
0.5	$Li_{1.0}Zn_{0.5}Al_{1.5}Fe_{0.5}O_4$	665.33		517.01
1.5	$Li_{1.0}Zn_{0.5}Al_{0.5}Fe_{1.5}O_4$	618.68		469.37
2	$Li_{1.0}Zn_{0.5}Fe_2O_4$	557.83	432.97	400.05

TABLE 4: Magnetic parameters of $Li_{1.0}Zn_{0.5}Fe_xAl_{2-x}O_4$ (x=0.0, 0.5, 1.5, 2.0) sintered at 1173K

| Fe content 'x'	Composition	Saturation Magnetization M_s (emu/g)	Remanent Magnetization M_r (emu/g)	Coercivity H_c (Oe)	Mr/Ms	Magneto Crystalline Anisotropy K (erg)	Magneton Number n_B
0	$Li_{1.0}Zn_{0.5}Al_2O_4$	0.298	0.1271	299.87	0.42651	89.36	0.008406
0.5	$Li_{1.0}Zn_{0.5}Al_{1.5}Fe_{0.5}O_4$	1.222	0.1229	29.3	0.10057	35.81	0.037629
1.5	$Li_{1.0}Zn_{0.5}Al_{0.5}Fe_{1.5}O_4$	80.072	47.1	5.78	0.58822	462.82	2.879517
2	$Li_{1.0}Zn_{0.5}Fe_2O_4$	37.298	8.9	2.67	0.23862	99.59	1.437679
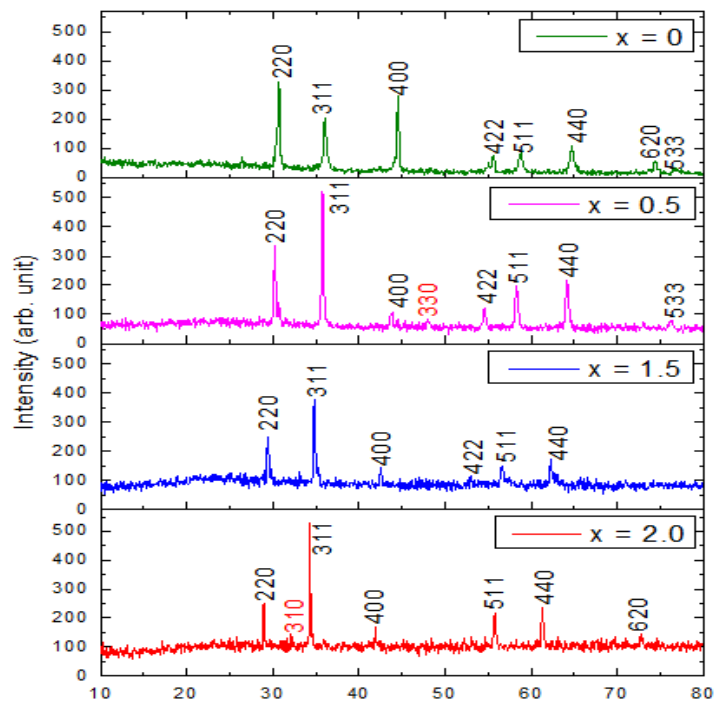
Figure 1: X-Ray Diffraction pattern of $Li_{1.0}Zn_{0.5}Fe_xAl_{2-x}O_4$ (x=0.0, 0.5, 1.5, 2.0) sintered at 1173K
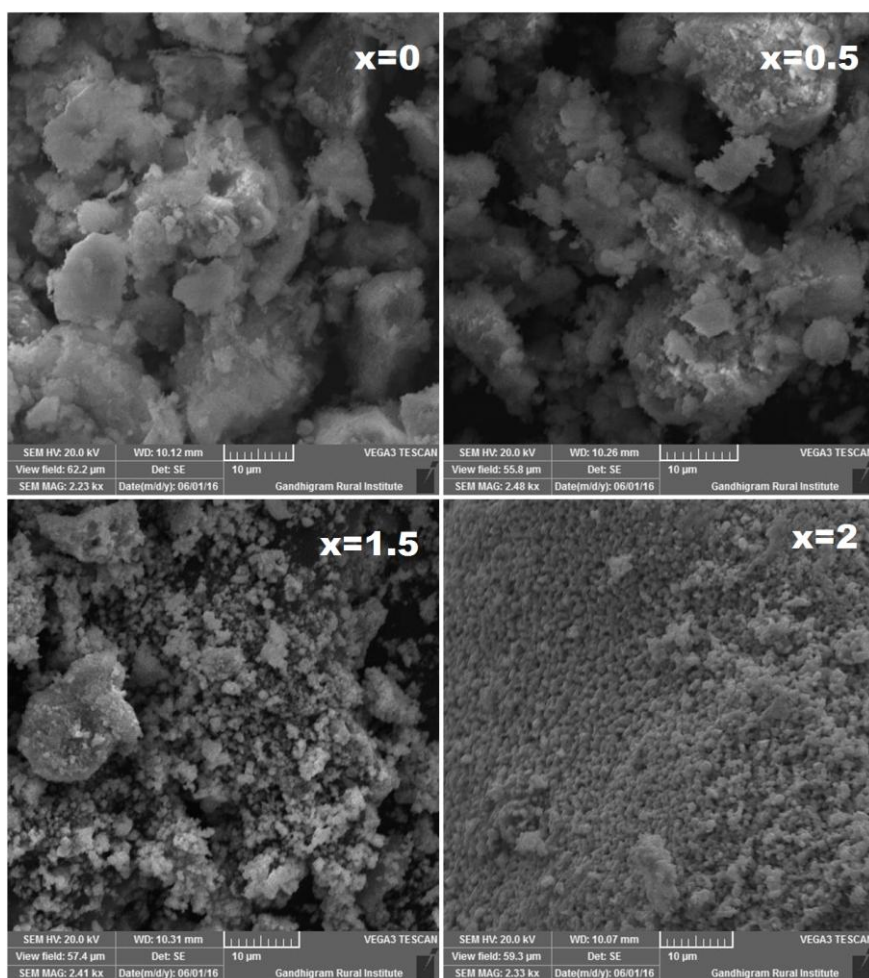

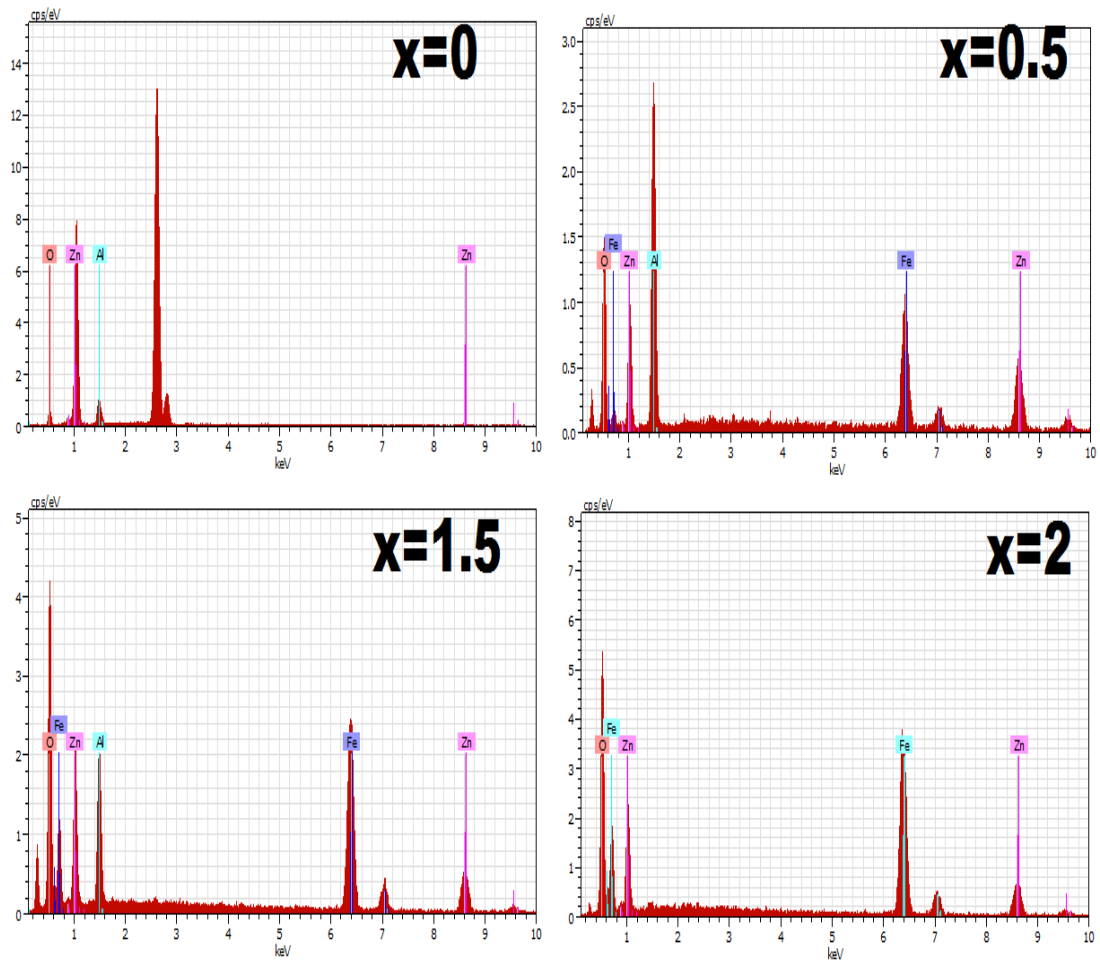Figure 2. SEM micrograph of $Li_{1.0}Zn_{0.5}Fe_xAl_{2-x}O_4$ (x=0.0, 0.5, 1.5, 2.0) sintered at 1173K

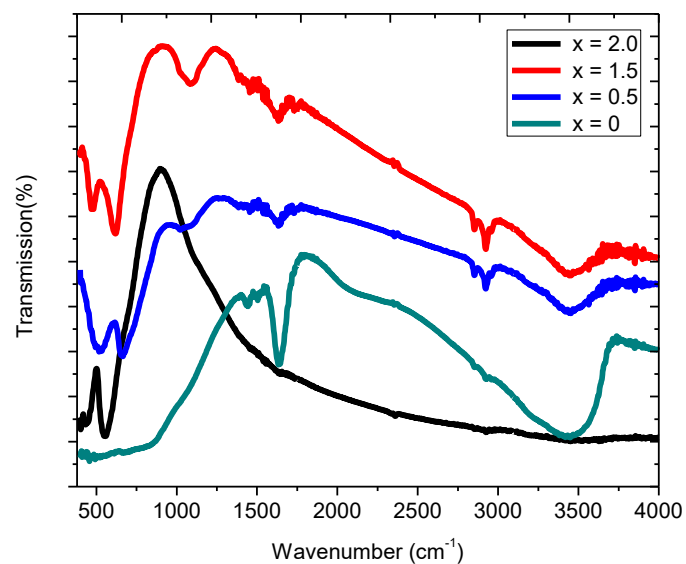Figure 3: EDS of $Li_{1.0}Zn_{0.5}Fe_xAl_{2-x}O_4$ (x=0.0, 0.5, 1.5, 2.0) sintered at 1173K

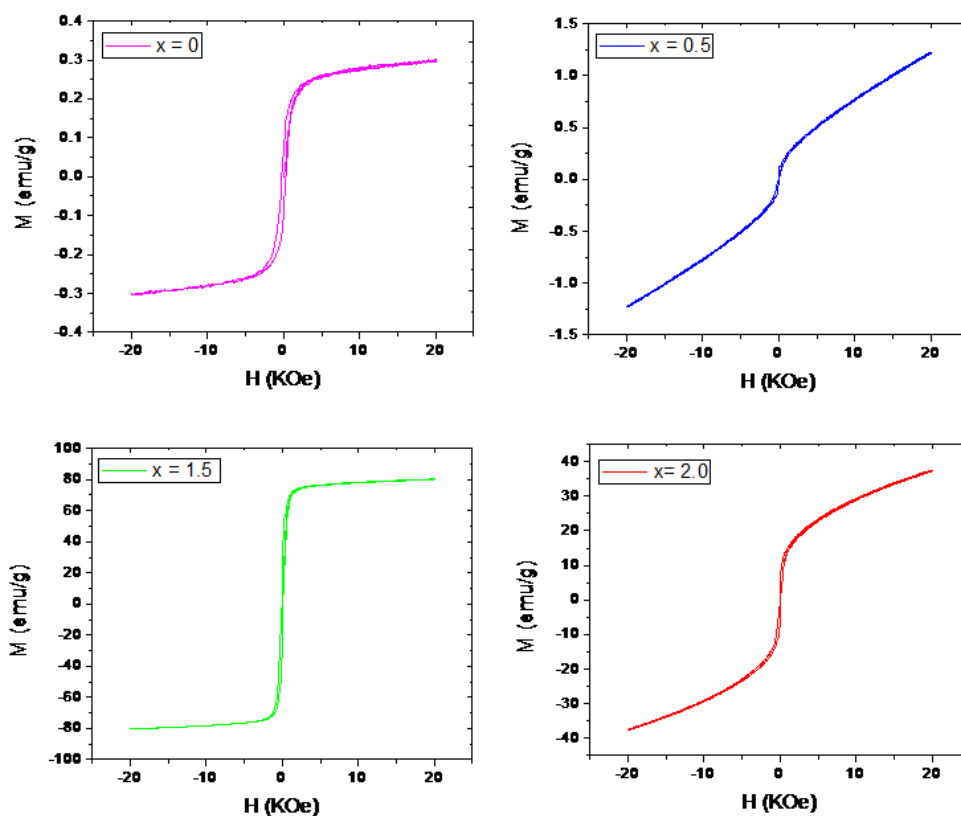Figure 4: FTIR spectra of $Li_{1.0}Zn_{0.5}Fe_xAl_{2-x}O_4$ (x=0.0, 0.5, 1.5, 2.0) sintered at 1173K

Figure 5: Magnetic hysteresis curves of $Li_{1.0}Zn_{0.5}Fe_xAl_{2-x}O_4$ (x=0.0, 0.5, 1.5, 2.0) sintered at 1173K